



Non-linear oceanic tides observed by superconducting gravimeters in Europe

Jean-Paul Boy^{a,c,*}, Muriel Llubes^b, Richard Ray^a, Jacques Hinderer^{a,c}, Nicolas Florsch^d, Séverine Rosat^c, Florent Lyard^b, Thierry Letellier^b

^a *Space Geodesy Branch, Code 926, NASA Goddard Space Flight Center, Greenbelt, MD 20771, USA*

^b *LEGOS/CNES/CNRS, 18 Avenue E. Belin, 31401 Toulouse Cedex, France*

^c *EOST-IPGS (UMR 7516), 5 rue René Descartes, 67084 Strasbourg, France*

^d *Département de Géophysique Appliquée, UMR 7619 Sysiphe, Université Pierre et Marie Curie, 4 Place Jussieu, 75252 Paris Cedex 05, France*

Received 24 December 2003; received in revised form 23 June 2004; accepted 9 July 2004

Abstract

We have analyzed data from nine superconducting gravimeters in Western Europe and detected the contribution of non-linear ocean tides in the quarter-diurnal and sixth-diurnal frequency bands. Despite their small amplitudes, a few nanogals ($10^{-11} \text{ m s}^{-2}$), we have compared the tidal loading observations with the loading effects inferred from several non-linear ocean tide models over the North-West European continental shelf and found that they are coherent with the recent models. We also confirmed our results with tide gauge data and Topex/Poseidon altimetric data.

We have also shown that the differences between the ocean tidal models are significantly larger than the accuracy of recent superconducting gravimeters. Therefore, we suggest that gravity measurements can be used as an independent validation tool for non-linear ocean tidal models, complementary to tide gauge and bottom pressure records.

© 2004 Published by Elsevier Ltd.

1. Introduction

Surface gravity measurements have been used to validate ocean tidal models in the diurnal and semi-diurnal frequency bands (see, for example, Baker and Bos, 2003; Boy et al., 2003) and also at longer

* Corresponding author.

E-mail address: jpboy@eost.u-strasbg.fr (J.-P. Boy).

periods (Bos et al., 2000). The loading contribution of non-linear oceanic tides has been clearly observed in gravity measurements using LaCoste–Romberg spring gravimeters (Baker, 1980a) and also in tilt measurements (Baker, 1980b), located in Great Britain where the amplitude can reach several tenths of microgals (10^{-8} m s^{-2}) in the vicinity of the Irish Sea. The high precision of superconducting gravimeter (SG) data allowed also the detection of small amplitude degree four lunar tidal waves in the quarter-diurnal frequency band (Florsch et al., 1995) for the Strasbourg (France) and Cantley (Canada) instruments, which are located a few hundred of kilometers from the coasts. A previous study by Merriam (1995) had shown that gravity measurements at Cantley are consistent with ocean tidal records in the Bay of Fundy with clear evidence for non-linear effects. Up to now however there is no direct validation of gravity observations with comparison with tidal models that incorporate the non-linear terms of the ocean tides in the North-West European shelf or the Bay of Fundy.

Improvements in ocean tidal modelling allow nowadays a precise representation of small amplitude waves, especially non-linear constituents, originating from interactions between principal diurnal and semi-diurnal waves on continental shelves, e.g. Sinha and Pingree (1997) and Andersen (1999). The amplitude of these tidal components can reach several tens of centimeters on major continental shelves, e.g. the North-West European shelf (Flather, 1976), the Patagonian (Glorioso and Flather, 1997) shelf or the Yellow Sea (Lefèvre et al., 2000).

Because non-linear tides over the North-West European continental shelf are well documented, and because there is a large number of superconducting gravimeter stations in Western Europe, we choose to extract a sub-network (see Fig. 1) of the Global Geodynamics Project (GGP) worldwide network (Crossley et al., 1999) of eight instruments. We also add the former series from SG T005 (Strasbourg, France) used by Florsch et al. (1995).

Non-linear oceanic tides over the North-West European shelf are modelled using Mog2D (2D Gravity Wave model) derived from Lynch and Gray (1979), a finite element, barotropic model solving the shallow water equations. It has been designed to provide accurate tidal simulations, using the state-of-the art techniques in this domain, like the parametrisation of the internal wave drag or the self-attraction and loading terms (Ray, 1998a).

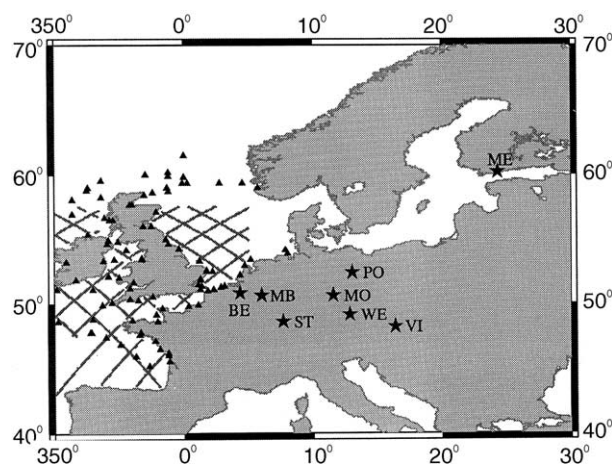


Fig. 1. Location of the eight GGP stations (asterisks), of the tide gauge network (triangles) used by Sinha and Pingree (1997) and Topex–Poseidon tracks.

In Section 2, we describe the processing of the SG data and show the results of our tidal analyses. Section 3 is devoted to the computation of non-linear ocean tidal loading using Mog2D. We show in Section 4 the comparison of different non-linear ocean tidal models over the European continental shelf with the SG records, but also with tide gauges and Topex-Poseidon altimetry. Concluding remarks are given in Section 5.

2. SG data processing

We analyzed SG data in a similar way as Florsch et al. (1995). Raw minute (or 5 min for SG T005) pressure and gravity data are first corrected for major perturbations, such as offsets due to acquisition failures, gaps or earthquakes by substituting a synthetic local tide. We then filtered them using a band pass filter with cut-off frequencies of 2.40 (10 h) and 8.64 (2.78 h) cycles per day and finally decimated to 1 h sampling. We give in Table 1 the location of all SG as well as the analyzed time period.

Some smaller amplitude perturbations are still present in the filtered gravity and pressure records. We therefore apply the same procedure for cleaning them, but with a smaller threshold than in the initial step. As shown by Fig. 2, it allows a significant reduction of the noise level in the sub-daily frequency bands.

Gravity data are then corrected for atmospheric loading effects and solid Earth tides. The atmospheric pressure contribution is modelled using a single admittance (Warburton and Goodkind, 1977) adjusted by least-square fitting between pressure and gravity. Solid Earth tides are modelled using Hartmann and Wenzel (1995) precise tidal potential and Dehant et al. (1999) gravimetric factors. Fig. 3 shows the spectrum of the gravity corrected for pressure effects, solid Earth tides and the gravity residuals for four recent instruments.

We can clearly identify in the gravity residual spectrum different peaks of a few nanogals, with the same frequency as some well known non-linear tides. In particular, we can see in all SG records a peak at the M4 frequency (3.865 cpd). Two other peaks in the quarter-diurnal frequency band can be found in most of SG data, at MN4 (3.828 cpd) and MS4 (3.932 cpd). For SGs close to the coast, we may also find two peaks in the sixth-diurnal band at M6 (5.797 cpd) and 2MS6 (5.865 cpd) frequencies, but with smaller amplitudes.

To obtain a more quantitative estimation of the amplitude and phase of all these peaks, we performed a tidal analysis of each of the SG residuals. Results are given in Table 2. The errors are not just formal errors, but are computed with an estimation of the noise level.

Table 1
Location and analyzed period of the eight superconducting gravimeters

	Latitude (°)	Longitude (°)	Period
BE	50.7986	4.3581	1997/07/13, 2000/09/09
MO	50.6450	11.6160	2000/01/13, 2001/11/20
MB	50.6093	6.0066	1995/08/16, 2000/07/19
ME	60.2172	24.3958	1994/08/28, 2000/12/19
PO	52.3806	13.0682	1994/08/13, 1998/08/19
ST	48.6217	7.6838	1987/07/22, 1996/06/13 ^a 1998/01/13, 2001/01/19 ^a
VI	48.2493	16.3579	1997/07/13, 2001/12/19
WE	49.1458	12.8794	1996/08/09, 1998/09/11

^a The two time series were recorded by the older T005 and the new CO26 instruments in Strasbourg (France).

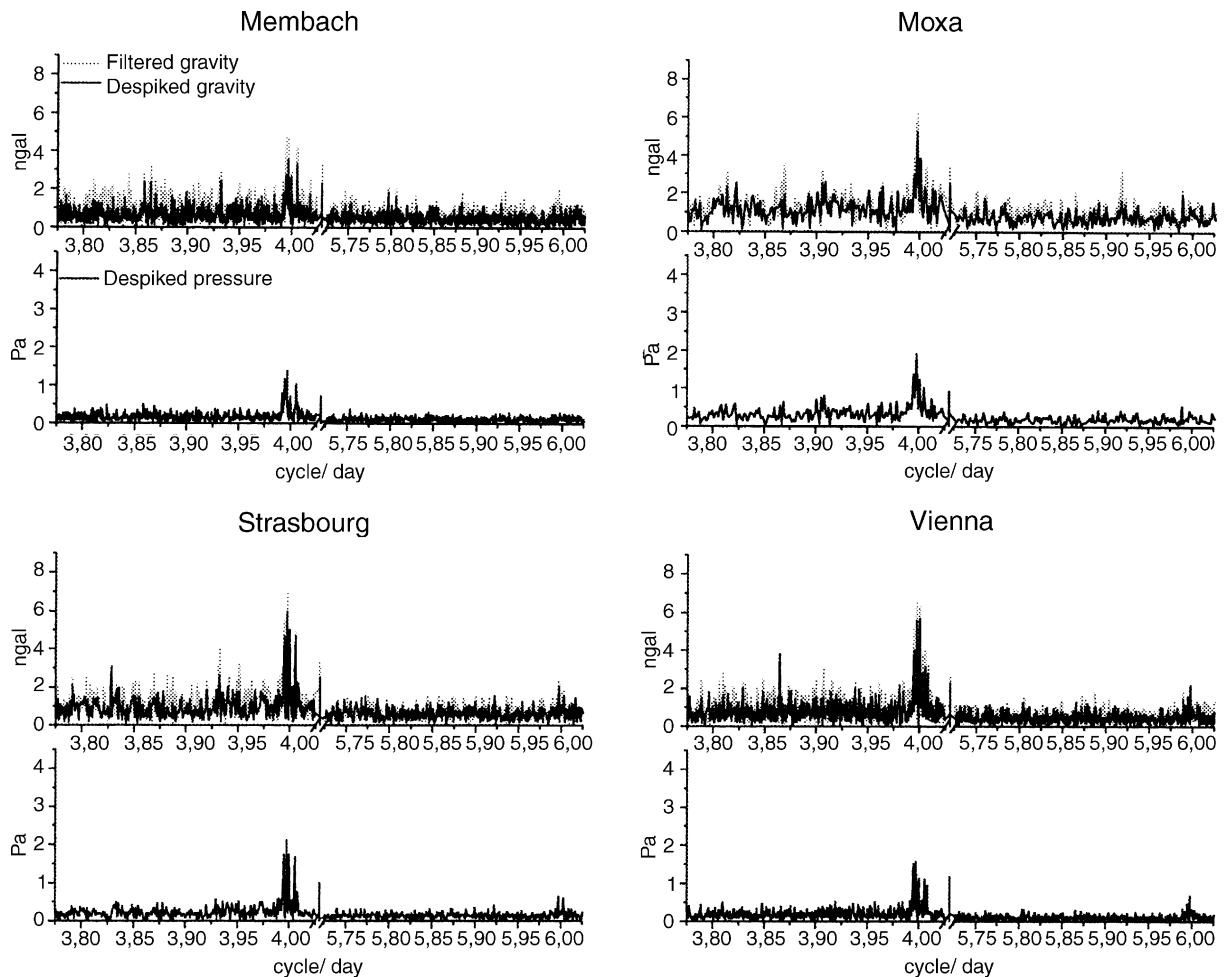


Fig. 2. Spectrum of the filtered and despiked gravity (top) and pressure (bottom) for SG CO21 in Membach (Belgium), CO26 in Strasbourg (France), CD034 in Moxa (Germany) and CO25 in Vienna (Austria).

The amplitudes of the quarter-diurnal tides reach a few nanogals ($10^{-11} \text{ m s}^{-2}$), with uncertainties of tenths of nanogals. For the sixth-diurnal tide M6, the amplitudes are smaller but still larger than the errors. Compared to the new instruments the old SG (BE, PO, ST-T005 and WE) produce twice as much noise at high frequencies.

3. Ocean tidal loading estimates

3.1. Generation of non-linear ocean tides

Eqs. (1) and (2) express the depth-integrated continuity and horizontal momentum equations derived from classical Navier–Stokes expression (Sinha and Pingree, 1997).

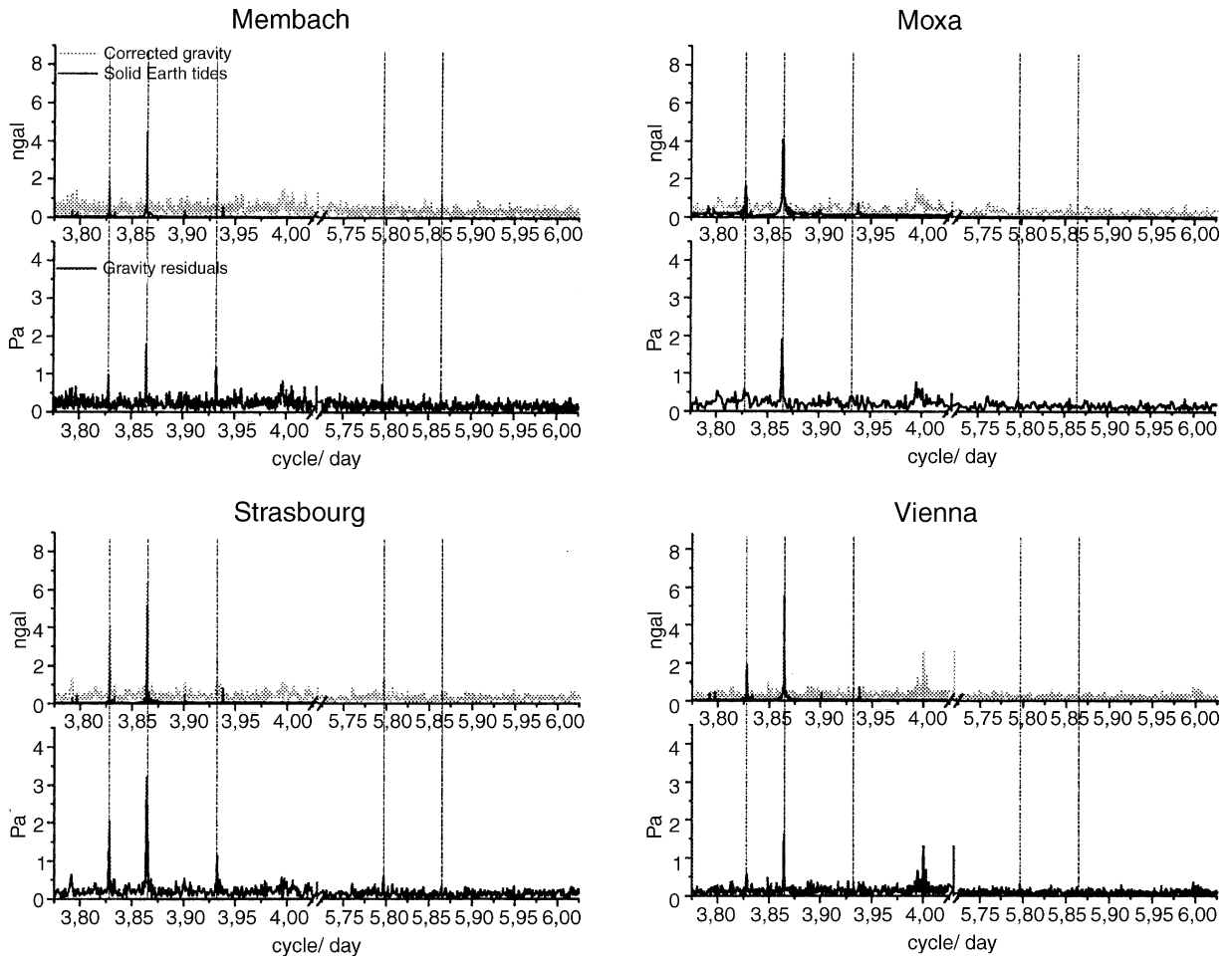


Fig. 3. Spectrum of gravity corrected for pressure effects and solid Earth tides (top) and observed ocean tidal loading for the same four stations. The vertical dot-dash lines shows the frequencies of major non-linear ocean tides.

$$\frac{\partial \eta}{\partial t} + \nabla(D\mathbf{u}) = 0 \tag{1}$$

$$\frac{\partial \mathbf{u}}{\partial t} + (\mathbf{u}\nabla)\mathbf{u} + 2\Omega \wedge \mathbf{u} = -g_0\nabla\eta - \frac{\tau_b}{\rho D} + k_H\nabla^2\mathbf{u} + \mathbf{F} \tag{2}$$

where η , \mathbf{u} and \mathbf{F} are the tidal sea height variations, horizontal velocity and the tide generating forces. D , ρ and Ω are the total sea depth (i.e. the sum of the undisturbed water depth and the tidal sea height variations η), the sea-water density and the angular velocity of the Earth’s rotation. τ_b and k_H are respectively the bottom stress and the coefficient of horizontal diffusion. Using this formalism, ocean self-attraction and loading (SAL) effects (Ray, 1998a) are neglected in Eqs. (1) and (2).

Non-linear ocean tidal components on continental shelves are induced by the non-linear terms in Eqs. (1) and (2), i.e. continuity equation (term $\nabla(D\mathbf{u})$), bottom friction (term $\tau_b/(\rho D)$) and spatial advection (term $(\mathbf{u}\nabla)\mathbf{u}$) of the principal diurnal and semi-diurnal tidals waves (Andersen, 1999). In particular, the

Table 2

Amplitude ($10^{-11} \text{ m s}^{-2}$) and phase (in degree with respect to Greenwich) of the observed non-linear ocean tidal loading

	MN4		M4		MS4		M6	
	Amplitude ($10^{-11} \text{ m s}^{-2}$)	Phase ($^{\circ}$)	Amplitude ($10^{-11} \text{ m s}^{-2}$)	Phase ($^{\circ}$)	Amplitude ($10^{-11} \text{ m s}^{-2}$)	Phase ($^{\circ}$)	Amplitude ($10^{-11} \text{ m s}^{-2}$)	Phase ($^{\circ}$)
BE	2.0 ± 0.4	128 ± 12	4.0 ± 0.4	220 ± 6	2.4 ± 0.4	324 ± 10	3.9 ± 0.3	155 ± 4
MO	1.7 ± 0.4	109 ± 13	3.9 ± 0.3	156 ± 5	1.1 ± 0.4	189 ± 18	0.7 ± 0.3	327 ± 21
MB	2.1 ± 0.3	104 ± 8	3.6 ± 0.3	173 ± 5	2.6 ± 0.3	300 ± 7	1.3 ± 0.3	147 ± 11
ME	0.9 ± 0.2	53 ± 14	2.6 ± 0.2	84 ± 5	0.8 ± 0.2	155 ± 16	0.2 ± 0.1	37 ± 40
PO	1.4 ± 0.4	101 ± 15	2.5 ± 0.7	141 ± 15	0.9 ± 0.4	173 ± 23	2.4 ± 0.3	107 ± 7
T005	3.3 ± 0.4	109 ± 6	7.5 ± 0.3	146 ± 3	2.1 ± 0.3	211 ± 9	0.3 ± 0.3	156 ± 54
CO26	4.1 ± 0.3	107 ± 4	7.0 ± 0.3	147 ± 3	2.3 ± 0.3	228 ± 7	1.4 ± 0.3	309 ± 11
VI	1.2 ± 0.2	96 ± 10	3.2 ± 0.2	141 ± 4	0.7 ± 0.2	193 ± 18	0.6 ± 0.2	52 ± 14
WE	1.4 ± 0.8	127 ± 32	4.7 ± 0.8	129 ± 10	1.0 ± 0.9	241 ± 50	3.7 ± 0.9	280 ± 15

non-linear quarter-diurnal wave M4 is generated by spatial advection of M2. The sixth-diurnal wave M6 comes from the friction term of M2.

3.2. Mog2D

Mog2D (2D Gravity Wave model) is a barotropic, non-linear and time stepping model, originally conceived by Lynch and Gray (1979) and developed since for coastal to global tidal and atmospheric driven applications. Model governing equations are based on the classical shallow water continuity and momentum equations. These are solved through a non-linear shallow-water wave equation with a quasi-elliptic formulation which improves numerical stability. The currents are derived through the non-conservative momentum equation. The model capabilities include tidal and meteorological forcing (atmospheric surface pressure and wind). Its main originality is a finite element space discretisation (FE), which allows increased resolution in regions of interest like high topographic gradient areas (showing strong current variability and internal waves generation) and shallow waters, where most of the bottom friction dissipation occurs. To improve the computational efficiency, a novel subcycling time-stepping scheme is dedicated to take care of unstable model nodes, allowing more generally to permit not only uneven spatial resolution but also locally variable time steps. Bottom friction is formulated using a Chezy-type quadratic parameterisation. In this case, the coefficient τ_b for the bottom friction term (see Eq. (2)) is equal to:

$$\tau_b = -\rho C_d \mathbf{u} |\mathbf{u}| \quad (3)$$

where C_d is a drag coefficient.

A novel parameterisation of the barotropic to baroclinic energy transfer (through the internal waves generation on topographic slopes) is included in the model. The horizontal viscosity is prescribed following the Smagorinsky viscosity scheme (Smagorinsky, 1963) which allows to take into account the varying FE mesh cells size. In essence, the barotropic model does not include any vertical energy dissipation (like ocean de-stratification processes or vertical shear drag), which appears to be a problem when the annual mean wind stress is kept in the simulation forcing. In this case, some unrealistically strong deep ocean circulations can appear. An additional rough Raleigh-type dissipation term is thus introduced in order to parameterise the internal dissipation (Egbert and Ray, 2000; Morozov, 1995).

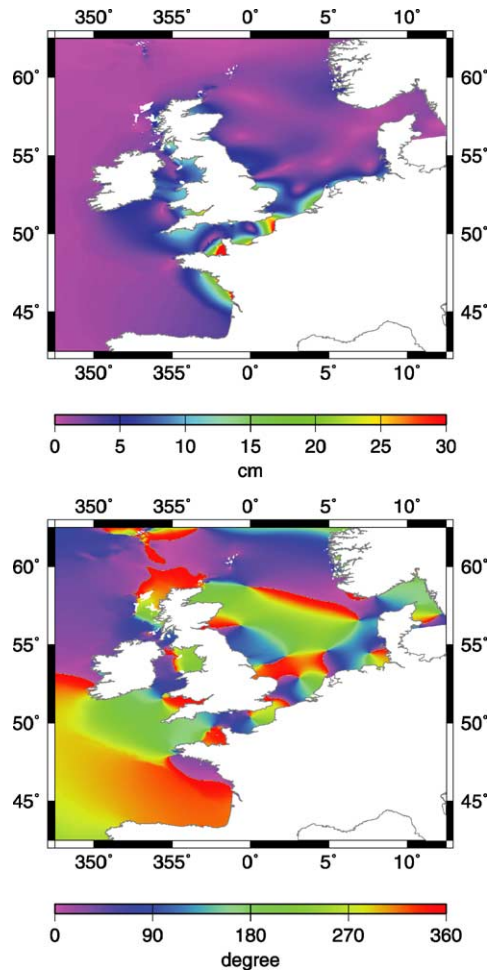


Fig. 4. Amplitude (cm) and phase ($^{\circ}$) of the M4 tidal wave over the North-West European continental shelf, according to Mog2D model.

The forcing is based on the astronomical and the self-attraction potential. Solid tide and tidal loading are also taken into account. An admittance method can optionally be activated to extend the computed tidal spectrum to the minor astronomical constituents. Boundary conditions are preferably extracted from available global simulations through a radiative condition (characteristics method). A two-step procedure improves the efficiency of this boundary condition when tidal elevation only are available for the boundary conditions and not the velocities. The Mog2D is currently used for global ocean atmospheric load modelling (to provide altimetry with accurate corrections for the ocean meteorologically forced dynamic), and to regional applications like the North-East Atlantic or the Mediterranean Sea, where both the tidal and storm surge dynamic are studied. A recent paper (in review) shows that the hydrodynamic tidal solutions obtained with Mog2D on regional models have an accuracy at least equivalent or better than the best available global models.

Table 3

Amplitude ($10^{-11} \text{ m s}^{-2}$) and phase (in $^{\circ}$) with respect to Greenwich) of the oceanic loading according to Mog2D tidal model

	MN4		M4		MS4		M6	
	Amplitude ($10^{-11} \text{ m s}^{-2}$)	Phase ($^{\circ}$)	Amplitude ($10^{-11} \text{ m s}^{-2}$)	Phase ($^{\circ}$)	Amplitude ($10^{-11} \text{ m s}^{-2}$)	Phase ($^{\circ}$)	Amplitude ($10^{-11} \text{ m s}^{-2}$)	Phase ($^{\circ}$)
BE	4.02	19.4	8.79	94.4	6.29	91.4	2.68	191.1
MO	1.28	87.1	7.32	142.9	1.52	165.5	0.50	65.4
MB	2.50	40.9	8.96	122.0	3.61	110.0	1.03	141.0
ME	0.56	145.6	3.49	163.3	0.78	232.0	0.40	29.2
PO	1.09	99.5	6.63	147.0	1.30	182.9	0.51	48.3
ST	2.12	80.5	11.39	141.4	2.55	158.5	0.67	94.2
VI	1.00	95.0	5.45	142.8	1.21	176.6	0.40	51.4
WE	1.25	90.2	6.96	142.8	1.50	170.5	0.46	60.2

Fig. 4 shows the M4 constituent over the European shelf, modelled by Mog2D. Compared to the diurnal and semi-diurnal tides, the non-linear shallow water constituents are characterized by small wavelengths. The maximum of M4 component occurs in the English Channel with amplitudes as large as 50 cm in the Bay of Mont Saint-Michel (for a detailed study of M4 tide in the English Channel, see Pingree and Maddock, 1978) whereas other tides reach typically 10–20 cm.

3.3. Loading estimates

The tidal loading is estimated with the classical Green's function approach (Farrell, 1972), i.e. by convolving the complex tidal height with Green's function (see, for example, Boy et al., 2003), computed for a spherically, symmetric, nonrotating, elastic, isotropic (SNREI) Earth model, and using PREM (Dziewonski and Anderson, 1981) elastic parameters. The tidal loading estimated with Mog2D ocean model is given in Table 3, for the waves MN4, M4, MS4 and M6, and for the eight stations.

Except for Brussels (Belgium), 70 km far from the North Sea coast and Metsahovi (Finland) (two old instruments), there is a good agreement (within the error bars) between loading estimates and observed tidal loading, both in phase and amplitude, except for the amplitude of M4 tidal wave.

4. Comparison of ocean tidal models

We have shown in the previous section that the observed ocean loading is coherent with the loading estimated with Mog2D model, at least for MN4, MS4 and even M6 components. However the modelled amplitude for M4 is typically twice the observed, although the phase is in good agreement.

We also wanted to compare the precision of gravity tidal records in the quarter and sixth-diurnal frequency bands to the difference between several tidal models. For example, the difference between tidal models for the eight main diurnal and semi-diurnal tides are usually larger than the precision of SG (see, for example, Boy et al., 2003).

We choose to focus on the major component M4, and to compare the loading effects estimated with Mog2D to an updated version of Flather (1976) and Pingree and Griffiths (1980, 1981) models. Unlike Mog2D, these two models are not purely hydrodynamic solutions, but also include assimilation of tide

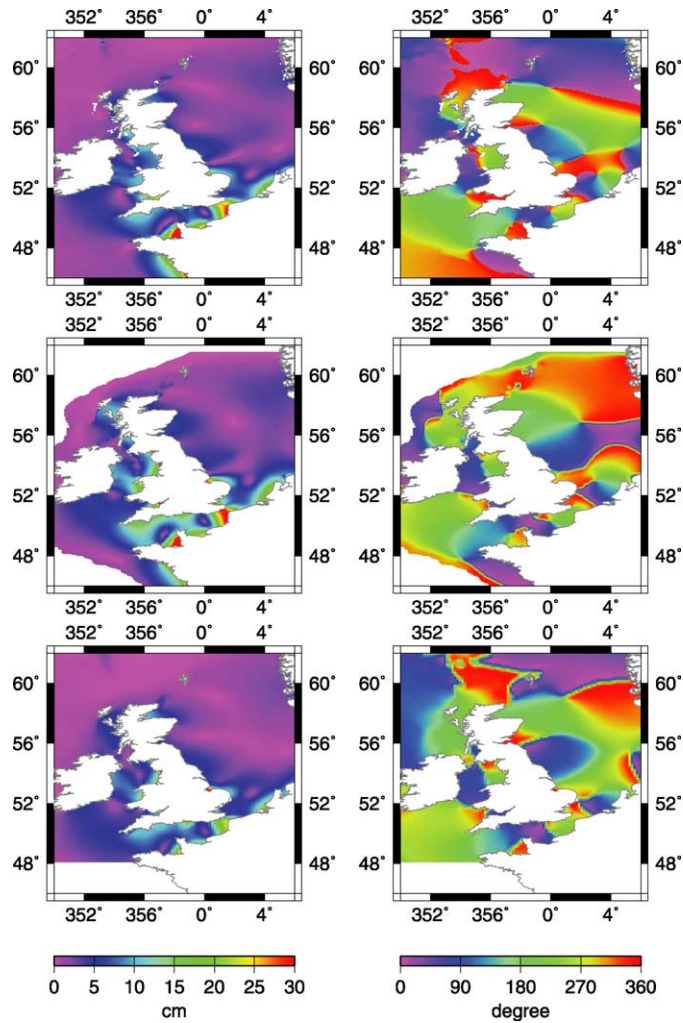


Fig. 5. Amplitude and phase of the M4 tidal waves from Mog2D (top), Pingree and Griffiths (1980, 1981) (middle) and the updated Flather (1976) (bottom) models.

gauge data. We also compared these models to direct tidal information from Topex/Poseidon (T/P) and tide gauges.

Fig. 5 shows the amplitude and phase of M4 tidal waves according to these three models. We can particularly notice higher amplitudes in the English Channel and the Irish Sea in the Pingree and Griffiths (1980, 1981) model compared to Mog2D, and also a phase difference of about 40° . In the North Sea, the three models are significantly different, although the amplitudes are quite small. This is especially true for the number (of their position) of the amphidromic points. We are comparing these models more quantitatively in the next two subsections to altimetry (T/P) and tide gauge data and to tidal gravity observations.

4.1. Topex/Poseidon and tide gauges

Andersen (1999) previously used T/P data to study non-linear tides over the European Shelf. He found that T/P data produced surprisingly accurate estimates of the M4 tide, but somewhat less satisfactory estimates for several other tides such as MS4 and M6. Andersen (1999) estimated the tides every 5.7 km along individual tracks and then employed statistical interpolation methods to produce a gridded tidal field with a resolution of 0.5° . We here follow a similar along-track estimation procedure, but we use those estimates directly for comparisons with our other tidal fields, without spatial interpolations or extrapolations. Our tidal estimates are based on ten years of T/P data.

As is well known, the 9.9156-day sampling of T/P aliases short-period tides to considerably longer periods. A fairly complete table of tidal aliased periods is given by Ray (1998b, Table 3). The aliased period of M4 is 31.1 days, which differs by at least one day from the aliased periods of other tidal constituents. M4 is thus easily separable from other constituents given the 10-year altimeter time series. On the other hand, M6 and L2 are aliased to nearly identical periods, and these two tides remain correlated in a 10-year time series and cannot be separated. The MS4 tide is aliased to about 3 years and is therefore susceptible to contamination from strong interannual oceanographic signals. We therefore restrict our attention here to the T/P results for M4.

A satellite altimeter is, of course, sensitive to the geocentric tide, the sum of body tide, ocean tide, and load tide. Being non-linear, M4 has no sensible body tide, but it does have a small associated load tide. Separation of ocean and load tides in altimeter tidal analyses is routinely done by an iterative procedure (Cartwright and Ray, 1991, Appendix A) with global data. Since we are here restricting our attention to a few tracks on the European Shelf, such a separation procedure is awkward and we here neglect it. Because the wavelengths of M4 on the shelf are short and loading Love numbers become small at high wavenumbers, the error of neglecting the M4 load tide correction is very small, of order 0.1 mm.

The standard errors in our along-track estimates of M4 are generally between 5 and 15 mm. The error estimates are based on an assumption of white noise, which is a reasonable assumption given (1) the long T/P sampling interval, which decorrelates successive observations, and (2) the fairly short M4 alias period, which minimizes background oceanographic noise. At a few locations, especially close to land, the standard errors exceed 2 cm. We have eliminated from our comparisons any estimate with a standard error exceeding 3 cm.

We also added in our comparison 99 tide gauge or bottom pressure records (Sinha and Pingree, 1997); their location are depicted in Fig. 1. We compute the root-mean-square (RMS) differences between the modelled and the observed (T/P or tide gauges) tidal height, but also the ratio between these RMS differences and the RMS of the observed sea tidal height (see Table 4).

Fig. 6 shows the definition of the different basins used in Table 4.

The comparison with tide gauges and T/P also shows a disagreement between M4 tidal wave modelled with Mog2D and tidal observations, except for the Gulf of Biscay. However this problem appears particularly for the amplitude, whereas the phases are usually in a better agreement. It is also not very surprising to observe a better agreement between Pingree and Griffiths (1980, 1981) and Flather (1976) models with tide gauge data and even T/P, due to the assimilation process of tide gauge data. Pingree and Griffiths (1980, 1981) solution appears to be the best model, with RMS differences of 5.53 cm with tide gauges and 2.22 cm with T/P estimates.

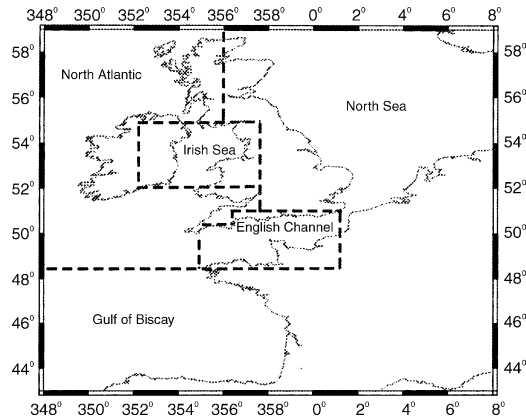


Fig. 6. Definition of the different basins (English Channel, Irish Sea, Gulf of Biscay, North Sea) used in the comparison of the ocean tidal models.

4.2. gravity changes

We also computed the M4 tidal loading effects from these two models for the seven gravity stations (see Table 5 and Fig. 7). Because the Gulf of Biscay is not present in the Flather (1976) shelf model and also because of its coarse resolution (0.11° in latitude and 0.17° in longitude), there is no agreement between this model and our loading estimates both in amplitude and phase. Similar to the comparison with tide gauges and altimetric data, we also retrieve a better agreement between the observed tidal loading and the loading estimated using the Pingree and Griffiths (1980, 1981) tidal model, even for the Brussels (BE) gravimeter located at 70 km from the North Sea coasts.

With respect to loading, we can also notice that the differences between the different non-linear tidal models are typically one order of magnitude larger than the accuracy of SG tidal observations, except for the Wettzell (WE) instrument. Both gravimeters installed in Strasbourg (ST) showed a large M4 tidal amplitude which are not confirmed by the loading estimated by any of the tidal models.

We also compute the loading contribution of the different shelf areas defined in Fig. 6 for five different stations. We can first notice that the disagreement between Flather (1976) model and SG observations is mainly due to the omission of the Gulf of Biscay.

Table 4
Comparison of M4 tidal models with tide gauges and bottom pressure

	Mog2D				Pingree and Griffiths (1980, 1981)				Flather (1976)			
	Tide gauges		Topex/Poseidon		Tide gauges		Topex/Poseidon		Tide gauges		Topex/Poseidon	
	Error	RMS	Error	RMS	Error	RMS	Error	RMS	Error	RMS	Error	RMS
European shelf	0.83	8.52	0.83	4.26	0.54	5.53	0.41	2.22	0.61	5.98	0.60	3.35
English Channel	0.85	12.63	0.96	7.66	0.42	6.20	0.38	2.99	0.48	7.19	0.52	4.19
Gulf of Biscay	0.69	9.32	0.46	1.75	0.73	9.82	0.40	1.52			(*)	
Irish Sea	0.74	6.73	0.63	3.77	0.38	3.46	0.33	1.96	0.55	5.12	0.53	3.19

RMS is given in cm, and the error values are the ratio of the RMS differences and the RMS of the observed sea height. (*) The grid of Flather (1976) shelf model stops at latitude 48.

Table 5

Amplitude ($10^{-11} \text{ m s}^{-2}$) and phase (in $^\circ$) with respect to Greenwich) of M4 tidal loading, according to Mog2D, Pingree and Griffiths (1980, 1981) and Flather (1976) models

	Mog2D		Pingree and Griffiths (1980, 1981)		Flather (1976)	
	Amplitude ($10^{-11} \text{ m s}^{-2}$)	Phase	Amplitude ($10^{-11} \text{ m s}^{-2}$)	Phase	Amplitude ($10^{-11} \text{ m s}^{-2}$)	Phase
BE	8.79	94.4	3.99	266.8	8.59	297.4
MO	7.32	142.9	3.35	147.6	1.86	41.9
MB	8.96	122.0	1.27	217.8	4.42	326.5
ME	3.49	163.3	2.73	137.0	0.35	111.6
PO	6.63	147.0	3.07	138.3	2.00	50.6
ST	11.39	141.4	4.88	158.9	2.82	41.4
VI	5.45	142.8	2.88	152.2	1.33	52.3
WE	6.96	142.8	3.42	152.8	1.71	47.8

As notice on Fig. 5, the North Sea’s contribution is different for all models and can also be significant for station close to the coasts (Membach, for example). There is no possibility to corroborate this result with T/P altimetry, as the amplitude of M4 is rather small, except along the English and Netherlands coasts.

We also retrieve the general conclusions found with the comparison with T/P altimetry and tide gauge data. The amplitude of M4 for Mog2D tidal model is larger in the Gulf of Biscay than for Pingree and Griffiths (1980, 1981) model; this is the opposite in the Irish Sea and the English Channel. There is also a phase shift between these two models, typically an advance of 40° for Mog2D in the Gulf of Biscay and for Pingree and Griffiths (1980, 1981) model in the English Channel.

It should be interesting to complete our study by including other tidal graviy records (from spring gravimeters, for example) especially closer to the coasts, where the ocean tidal contribution can be one order of magnitude larger (Table 6).

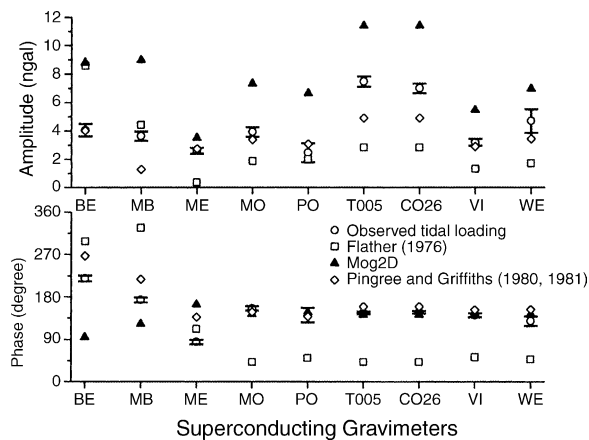


Fig. 7. Amplitude (in nanogal) and phase (in degree with respect to Greenwich) of M4 observed tidal loading and the estimated loading according to Flather (1976), Mog2D and Pingree and Griffiths (1980, 1981) tidal models.

Table 6
Comparison of the M4 loading effects induced by the different basins for 5 different SGs

		English Channel		Gulf of Biscay		North Sea		Irish Sea		North Atlantic	
		ngal	°	ngal	°	ngal	°	ngal	°	ngal	°
MO	Mog2D	1.07	289.2	6.52	147.3	0.55	98.6	0.37	220.3	1.22	92.9
	Pingree and Griffiths (1980, 1981)	1.59	244.8	4.69	194.3	1.43	73.6	0.94	217.8	4.16	52.6
	Flather (1976)	1.65	251.2	0.40	50.3	0.12	97.3	0.83	247.8	3.63	53.7
MB	Mog2D	2.01	285.9	10.99	153.0	5.18	24.8	0.63	223.7	2.15	78.8
	Pingree and Griffiths (1980, 1981)	2.48	245.6	7.96	195.2	4.76	349.7	1.55	218.2	6.21	50.9
	Flather (1976)	2.78	253.4	0.65	50.0	4.22	290.2	1.39	249.5	5.56	55.4
ME	Mog2D	0.43	299.0	2.44	139.3	0.97	217.1	0.16	212.2	0.71	148.2
	Pingree and Griffiths (1980, 1981)	0.68	251.2	1.69	194.5	1.59	134.3	0.46	216.8	2.31	57.9
	Flather (1976)	0.66	255.3	0.17	50.7	1.00	195.8	0.42	244.7	1.82	49.5
ST	Mog2D	1.58	280.1	10.50	152.5	1.75	78.3	0.53	225.8	1.87	75.4
	Pingree and Griffiths (1980, 1981)	2.21	238.9	7.65	194.1	2.50	55.0	1.22	219.7	5.06	49.4
	Flather (1976)	2.42	247.6	0.56	50.0	0.81	50.5	1.07	249.0	4.58	55.3
VI	Mog2D	0.69	290.5	4.68	144.1	0.41	148.9	0.27	222.0	0.89	93.3
	Pingree and Griffiths (1980, 1981)	1.08	245.7	3.42	193.7	1.06	100.1	0.65	218.9	2.93	52.3
	Flather (1976)	1.11	251.1	0.29	50.4	0.30	135.1	0.57	247.4	2.55	53.7

5. Results and discussion

The high accuracy of SG measurements allows the detection of loading effects induced by the major compound tides over the North West European continental shelf, in the quarter and also sixth-diurnal frequency bands, even for a station like Vienna (VI) 800 km far from the North Sea coasts. Their amplitudes reach several nanogals ($10^{-11} \text{ m s}^{-2}$), with a precision of about a few tenths of nanogal. We have shown that the SG observations are quantitatively coherent with tidal loading estimated with different shelf models, and also that the differences between these models are larger than the accuracy of most superconducting gravimeters.

We have also seen that it is very difficult to extract other components than M4 in altimetry. Therefore, the only oceanographic data which could be used for validating non-linear ocean tidal models over the North West European continental shelf are tide gauges. However these instruments are often installed at coastal stations and may only be representative of very local effects. Therefore high accuracy gravity measurements is one of the few methods to validate non-linear ocean tidal models on larger spatial scales. We also would like to extend our comparison between tidal models to other constituents (mainly MN4, MS4, M6 and eventually 2MS6) and also to other models.

It should be interesting to add other gravity records, from spring meters for example, especially in the vicinity of the Irish Sea. In this region, the amplitude of non-linear tidal waves are not only important, but the differences between models are also larger. For example, we found that the loading in Llanrwst, North Wales (Baker, 1980a,b) is equal to 12.1 nanogals and 171° , and respectively 21.6 nanogals and 280 degree for Pingree and Griffiths (1980, 1981) and Mog2D models.

Although GGP is a global worldwide network, it is really difficult to extend our study to other continental shelves. There is no gravimeter near the Patagonian shelf (Glorioso and Flather, 1997). Lefèvre et al. (2000) also computed M4 and MS4 waves in the Yellow Sea, in the vicinity of the three Japanese stations (Esashi, Kyoto and Matsushiro) and the Chinese gravimeter (Wuhan). However the distance of these gravimeters to the Yellow Sea is larger than the distance from the European gravimeters to the North Sea coast and therefore the induced loading should be smaller.

Acknowledgment

We acknowledge GGP members (<http://www.eas.slu.edu/GGP/ggphome.html>) for providing gravity and pressure data to the data base (<http://www.etggp.oma.be>) located at ICET (International Center of Earth Tides) at Brussels (Belgium). We also thank all oceanographers and ocean tide modellers for providing their models. We thank H.-G. Scherneck and an anonymous referee for their comments and suggestions that helped in improving the manuscript.

References

- Andersen, O.B., 1999. Shallow water tides in the northwest European shelf region from Topex/Poseidon altimetry. *J. Geophys. Res.* 104 (C4), 7729–7741.
- Baker, T.F., 1980. Tidal gravity in Britain: tidal loading and the spatial distribution of the marine tide. *Geophys. J.R. Astron. Soc.* 62, 249–267.
- Baker, T.F., 1980. Tidal tilt at Llanrwst, North Wales: tidal loading and Earth structure. *Geophys. J.R. Astron. Soc.* 62, 269–290.
- Baker, T.F., Bos, M.S., 2003. Validating Earth and ocean tide models using tidal gravity measurements. *Geophys. J. Int.* 152, 468–485.
- Bos, M.S., Baker, T.F., Lyard, F.H., Zürn, W.E., Rydelek, P.A., 2000. Long-period lunar Earth tides at the geographic South Pole and recent models of ocean tides. *Geophys. J. Int.* 143, 490–494.
- Boy, J.-P., Llubes, M., Hinderer, J., Florsch, N., 2003. A comparison of tidal ocean loading models using superconducting gravimeter data. *J. Geophys. Res.* 108, 2193, doi:10.1029/2002JB002050.
- Cartwright, D.E., Ray, R.D., 1991. Energetics of global ocean tides from Geosat altimetry. *J. Geophys. Res.* 96, 16897–16912.
- Crossley, D.J., Hinderer, J., Casula, G., Francis, O., Hsu, H.T., Imanishi, Y., Jentzsch, G., Kääriäinen, J., Merriam, J., Meurers, B., Neumeier, J., Richter, B., Shibuya, K., Sato, T., van Dam, T.M., 1999. Network of superconducting gravimeters benefits a number of disciplines. *Eos Transact.* 80, 121–126.
- Dehant, V., Defraigne, P., Wahr, J.M., 1999. Tides for a convective Earth. *J. Geophys. Res.* 104 (B1), 1035–1058.
- Dziewonski, A.M., Anderson, D.L., 1981. Preliminary Reference Earth Model. *Phys. Earth Planet. Inter.* 25, 297–356.
- Egbert, G.D., Ray, R.D., 2000. Significant dissipation of tidal energy in the deep ocean inferred from satellite altimeter data. *Nature* 405, 775–778.
- Farrell, W.E., 1972. Deformation of the Earth by surface loads. *Rev. Geophys. Space Phys.* 10, 761–797.
- Flather, R.A., 1976. A tidal model of the North-West European continental shelf. *Mém. Soc. R. Soc. Liège* 9, 141–164.
- Florsch, N., Hinderer, J., Legros, H., 1995. Identification of quarter diurnal waves in superconducting gravimeter data. *Bull. Inf. Marées Terr.* 122, 9189–9198.
- Glorioso, P.D., Flather, R.A., 1997. The Patagonian Shelf tides. *Prog. Oceanog.* 40, 263–283.
- Hartmann, T., Wenzel, H.G., 1995. The HW95 tidal potential catalogue. *Geophys. Res. Lett.* 22 (24), 3553–3556.
- Lefèvre, F., Le Provost, C., Lyard, F.H., 2000. How can we improve a global ocean tide model at a regional scale? A test on the Yellow Sea and the East China Sea. *J. Geophys. Res.* 105, 8707–8725.
- Lynch, D.R., Gray, W.G., 1979. A wave equation model for finite element tidal computations. *Comput. fluids* 7, 207–228.

- Merriam, J.B., 1995. Non-linear tides observed with the superconducting gravimeter at Cantley, Quebec. *Geophys. J. Int.* 123, 529–540.
- Morozov, E., 1995. Semidiurnal internal wave global field. *Deep Sea Res.* 42, 135–148.
- Pingree, R.D., Maddock, L., 1978. The M4 tide in the English Channel derived from a non-linear numerical model of the M2 tide. *Deep Sea Res.* 25, 53–63.
- Pingree, R.D., Griffiths, K.D., 1980. Currents driven by a steady uniform windstress on the shelf seas around the British Isles. *Oceanol. Acta* 3, 227–235.
- Pingree, R.D., Griffiths, K.D., 1981. S2 tidal simulations on the North-West European Shelf. *J. Mar. Biol. Assoc. UK* 61, 609–616.
- Ray, R.D., 1998a. Ocean self-attraction and loading in numerical tidal models. *Marine Geod.* 21, 181–192.
- Ray, R.D., 1998b. Spectral analysis of highly aliased sea-level signals. *J. Geophys. Res.* 103, 24991–25003.
- Sinha, B., Pingree, R.D., 1997. The principal lunar semidiurnal tide and its harmonics: baseline solutions for M2 and M4 constituents on the North-West European continental shelf. *Cont. shelf Res.* 17, 1321–1365.
- Smagorinsky, J., 1963. General circulation experiments with the primitive equations. *Monthly Weather Rev.* 91, 99–164.
- Warburton, R.J., Goodkind, J.M., 1977. The influence of barometric pressure variations on gravity. *Geophys. J.R. Astron. Soc.* 48, 281–292.